ELSEVIER

Blood 142 (2023) 715–717

The 65th ASH Annual Meeting Abstracts

ORAL ABSTRACTS

603.LYMPHOID ONCOGENESIS: BASIC

Classic Hodgkin Lymphomas Display Neuronal-Glial Lineage Transdifferentiation

Mirca S. Saurty-Seerunghen, PhD[1], Sara Moein, PhD[1], Tsega-Ab Abera[1], Xiaotian Sun[2], Sohani Sharma[1], Chhiring Lama[1], Mansi Totwani[1], Shira Rosenberg, MSc[1], Qi Gao, DCLS[2], Neelang Parghi[3], Amy Chadburn, MD[4], Kui Nie, PhD[1], Vicenta Trujillo Alonso[1], Elizabeth Bier[1], Jenny Xiang[1], Ethel Cesarman, MDPhD[1], Wayne Tam, MD[5], Mikhail Roshal, MD PhD[2], Lisa Giulino Roth, MD[1], Anna S Nam, MD[1]

[1] Weill Cornell Medicine, New York
[2] Memorial Sloan Kettering Cancer Center, New York
[3] New York University, New York
[4] Northwestern School Feinberg School of Medicine Northwester Memorial Hospital, New York, NY
[5] Northwell Health, New York

The molecular drivers of classic Hodgkin lymphoma (HL) underlying its pathologic and clinical distinctions from non-Hodgkin lymphoma (NHL) have been challenging to uncover. The study of HL has been impeded by the rarity of the Hodgkin-Reed-Sternberg (HRS) cells within a dense tumor microenvironment (TME). Previously, we developed a FACS approach to isolate the HRS cells and profiled their whole exomes and genomes (Reichel et al 2015; Maura et al 2023). These studies did not reveal an HRS-specific mutational signature, but rather mutations that overlap with those of NHL, such as those in *SOCS1* and *HIST1H1E*. These data suggested that non-genetic factors such as the underlying cell state may cooperate with somatic mutations to induce HL. However, we previously lacked the ability to co-map somatic mutations and cell states within the same cancer cells. We thus developed Genotyping of Transcriptomes (GoT; Nam et al 2019) that links single-cell RNA-seq (scRNA-seq) and somatic mutations within the same thousands of individual cells. We applied GoT to primary HL samples (n = 10 HL; 68291 cells, Fig. 1A) after FACS-isolation of HRS cells.

We analytically integrated the cells across the samples based on gene expression and identified the expected cell types including B-cells, T-cells, monocytes and HRS cells (Fig. 1B). As expected, the HRS cells displayed low expression of B-cell antigens (*CD19*, *CD79A*) and high levels of *TNFRSF8* (CD30), *CCL17*, *CCR7* and *PD-L1* (Fig. 1C). GoT data revealed that mutations were restricted to the HRS cells (Fig. 1D). Copy number variation (CNV) analysis further confirmed that CNVs were specific to the HRS cells (Fig. 1E).

As scRNA-seq has unveiled marked intratumoral cell state heterogeneity across cancers, we posited that the HRS cells may display heterogeneous cell states. Indeed, we identified distinct cell states (Fig. 1F), including cycling HRS and metabolically-active HRS cells upregulating the translation machinery (*NACA*, *RACK1*). We also observed a cell state with elevated inflammatory signals (*TNF*, *JUN*, *FOS*, *CCL22*). One group demonstrated a partially preserved B cell program with high *CD19* and *CD79A*. Unexpectedly, we also identified an HRS state with features of neuronal-glial (NG) transdifferentiation, including genes involved in synapse formation (*NRG2*, *NRXN3*). Consistently, genes upregulated in the NG state were enriched in nervous system and neuronal development pathways (Fig. 1G). We further assessed NG gene expressions across normal cell types and confirmed their specificity to NG lineage cells (Fig. 1H). These findings were consistent with dendritic processes of HRS cells highlighted by CD15 and CD30 (Fig. 1I, red arrows). Areas of CD15/CD30 staining devoid of nucleus (Fig. 1I, blue arrows) corroborated the presence of dendritic processes. These results suggested that the NG differentiation may be a key defining feature of HRS cells, whereby dendritic processes facilitate a tight control of the TME. Consistently, we identified strong HRS-immune complexes that persisted through tissue processing and sorting (Fig. 1F).

To determine the degree of plasticity or heritability of the HRS cell states, we integrated VDJ sequencing with GoT (GoT-VDJ), whereby somatic hypermutations in the VDJ served as endogenous barcodes. Phylogenetic reconstructions revealed that HRS cell states were distributed across clades (Fig. 1J), unveiling a plastic interchange of HRS cell states. Consistently, GoT showed that mutant cells were present across the cell states (Fig. 1K), indicating that the cell states were decoupled from the genetic identities.

We therefore postulated that the NG program may be encoded epigenetically. We performed single nuclei ATAC-seq on HRS-enriched HL samples (n = 5 samples; Fig. 1L). Compared to admixed B cells, the HRS cells displayed enhanced accessibility for

binding motifs of the NG lineage transcription factors (TF), e.g. OLIG1/2 and SOX family (Fig. 1M), revealing the TF networks that govern the lineage infidelity program. We further identified that the NG program is cell intrinsic and at least partially stable through *in vitro* passaging, as 4 of 5 HL cell lines exhibited the highest NG gene expression compared to NHL cell lines (Fig. 1N).

Altogether, these single-cell multi-omics studies indicated that an epigenetically encoded NG program may cooperate with lymphoma driving mutations to drive the development of HL, paving novel avenues of therapy.

Disclosures Chadburn: *Leica Biosystems:* Consultancy; *Boehringer Ingelheim Pharmaceuticals, Inc.:* Consultancy; *Medical College of Wisconsin:* Honoraria. **Roshal:** *Beat AML:* Other: Funding; *Physicians' Education Resource:* Other: Provision of services; *NGM:* Other: Funding; *Roche:* Other: Funding; *Celgene:* Other: Provision of services; *Auron Therapeutics:* Other: Ownership/Equity interests; Provision of services. **Roth:** *Roche:* Consultancy, Membership on an entity's Board of Directors or advisory committees; *Merck:* Consultancy, Membership on an entity's Board of Directors or advisory committees.

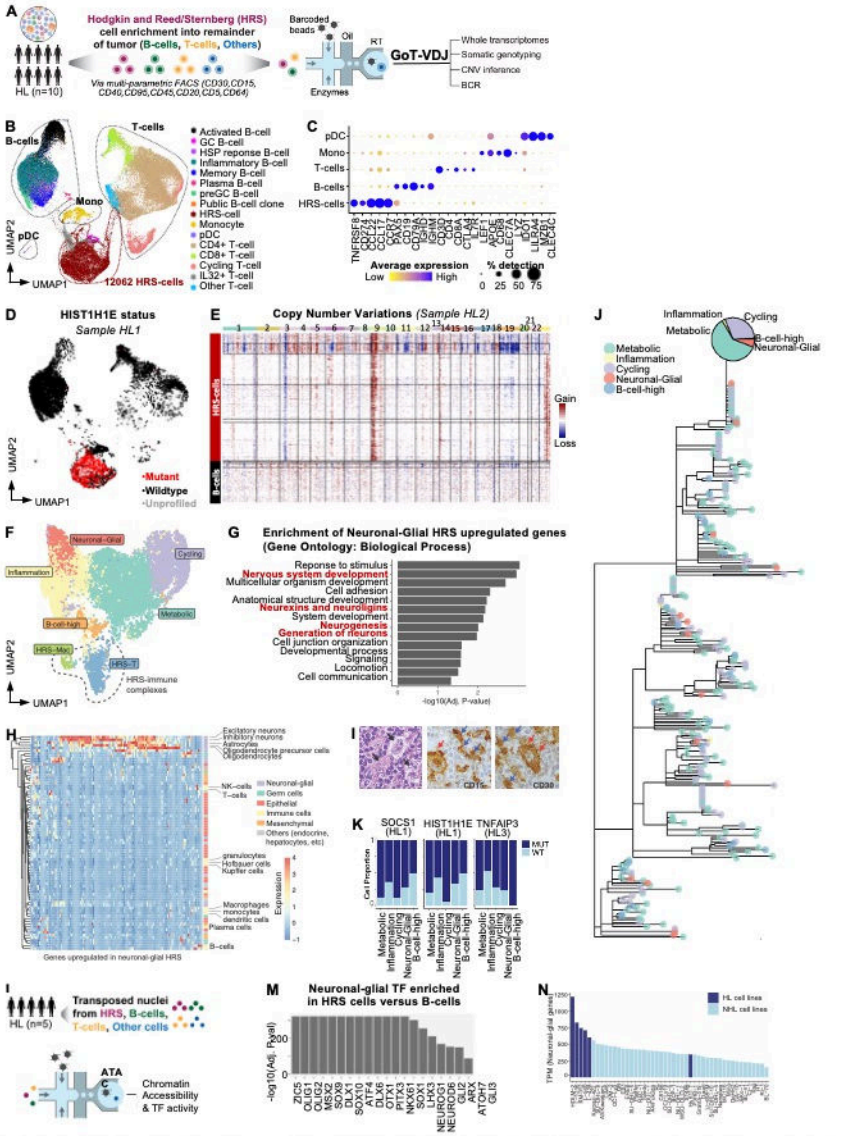

Figure 1. A. Schematic of GoT-VDJ. For each classic Hodgkin Lymphoma (HL) sample, FACS-sorted Hodgkin-Reed-Sternberg (HRS)-cells, B-cells, T-cells and unsorted cells are pooled together into one Genotyping of Transcriptomes (GoT) experiment (Nam et al 2019) integrating B-cell Receptor sequencing (GoT-BCR) for capturing somatic mutations, trancriptional profiles and BCR profiles from the same cell. **B.** Uniform Manifold Approximation and Projection (UMAP) of cell types identified upon clustering cells based on transcriptomic profiles (Seurat integration workflow, n=10 cHL). Mono: monocyte, pDC: plasmacytoid-Dendritic Cell, GC: Germinal Center. **C.** Dot plot showing mean normalized expression of genes known to be highly expressed in HRS cells or immune cells. **D.** UMAP projection of cells with wild-type or mutant form of HIST1H1E gene from HL1 sample. Representative sample with genotyping data shown. **E.** Heatmap of modified expression in HRS-cells and B-cells across the chromosomes with normal T-cells and myeloid cells as reference, for copy number variation (CNV) analysis (InferCNV package). Representative patient sample shown. CNV analysis inferred from the whole transcriptomic data . **F.** UMAP of HRS cells, which are a subset of the original dataset and have been reclustered, showing several distinct clusters based on scRNA-seq data (n= 12062 HRS cells, 10 patients). HRS-T: HRS-Tcell complex, HRS-Mac: HRS-Macrophage complex. **G.** Gene set enrichment analysis of genes upregulated in the neuronal-glial HRS-cell state. Neuronal processes are highlighted in red. **H.** Heatmap showing expression levels of genes upregulated in the neuronal-glial HRS-cell state across human cell types. **I.** H&E (left panel) and immunohistochemical staining for HRS markers CD15 and CD30 (middle and right panels, respectively) in one representative cHL tissue. Black arrows highlight HRS-cells, red arrows show dendritic processes while blue arrows show areas of cytoplasmic CD15/CD30 staining devoid of nucleus. **J.** Representative phylogenetic tree based on somatic hypermutations introduced to the light-chain VJ sequences across HRS-cells. Branch tips colored by HRS cell states as in Fig. 1F. **K.** Barplot showing proportion of HRS cells in each cell state bearing mutations in SOCS1, HIST1H1E or TNFAIP3 in representative samples. **L.** Schematic of ATAC. **M.** Barplot showing selected transcription factors involved in neuronal-glial functions and enriched in HRS cells compared to B-cells. **N.** Barplot showing expression of neuronal-glial genes across HL and non-HL cell lines. Bulk gene expression data for cell lines from The Human Protein Atlas.

Figure 1

https://doi.org/10.1182/blood-2023-189533